

Detection of the Vorticity Effect on the Disk Orientations

Jounghun Lee

Department of Physics and Astronomy, Seoul National University, Seoul 151-747, Korea

jounghun@astro.snu.ac.kr

ABSTRACT

We present an observational evidence for the vorticity effect on the nonlinear evolution of the galaxy angular momentum. We first calculate the vorticity as the curl of the peculiar velocity field reconstructed from the 2MASS redshift survey. Then, measuring the alignments between the vorticity and the tidal shear fields, we study how the alignment strength and tendency depends on the cosmic web environment. It is found that in the knot and filament regions the vorticity vectors are anti-aligned with the directions of the maximal volume compression while in the void and sheet regions they are anti-aligned with the directions of the minimal compression. Determining the spin axes of the nearby large face-on and edge-on disk galaxies from the Seventh Data Release of the Sloan Digital Sky Survey and measuring their correlations with the vorticity vectors at the galaxy positions, we finally detect a clear signal of the alignments between the galaxy spin and the local vorticity fields. The null hypothesis that there is no alignment between them is rejected at the 99.999% confidence level. Our result supports observationally the recently proposed scenario that although the galaxy angular momentum originates from the initial tidal interaction in the linear regime its subsequent evolution is driven primarily by the cosmic vorticity field.

Subject headings: cosmology:theory — large-scale structure of universe

1. INTRODUCTION

The most prevalent theory for the origin of the galaxy spins is the tidal torque theory which explains that a galaxy acquired its spinning motion (i.e., the angular momentum) via the tidal interaction with the surrounding matter fluctuations at its proto-galactic stage (Peebles 1969; Doroshkevich 1970; White 1984). One of the key predictions of the tidal torque theory is the existence of the local correlations between the galaxy spin and the tidal shear fields (Catelan & Theuns 1996a,b; Lee & Pen 2000; Pen et al. 2000; Lee & Pen

2001; Porciani et al. 2002a,b): The initial tidal torques which lasted till the turn-around moments caused the alignments between the spin axes of the proto-galaxies and the intermediate principal axes of the linear tidal fields. In the subsequent evolution the initially established spin-shear alignments would become weaker as the non-linear effects like galaxy-galaxy interactions should play a role of randomizing the galaxy spin axes (Dubinski 1992; Catelan & Theuns 1996b; Crittenden et al. 2001, 2002; Porciani et al. 2002a; Lee & Pen 2002, 2008).

Plenty of observational evidences have been found for the existence of the intrinsic spin-shear correlations (Schäfer 2009, for a comprehensive review). For instance, Lee & Erdogdu (2007) provided a direct observational evidence for the existence of the intrinsic spin-shear correlations by using the tidal shear fields reconstructed from the 2MASS redshift survey (Erdoğdu et al. 2006) and the galaxy catalog compiled by B. Tully (Pen et al. 2000). However, even though the main result of Lee & Erdogdu (2007) was seemingly consistent with the prediction of the linear tidal torque theory, they noted that the detected environmental dependence of the spin-shear alignments could not fit well into the tidal torque picture. The nonlinear effects which would destroy the initially established spin-shear alignments should be stronger in denser environments. Therefore, in the tidal torque picture, the galaxies located in denser regions were expected to show weaker spin-shear alignments. In contrast, what was found by Lee & Erdogdu (2007) was an opposite trend that the galaxies located in denser environments exhibit stronger intrinsic spin-shear alignments (see Figure 6 in Lee & Erdogdu 2007).

A similar trend was also detected by Lee (2011) who measured the spin-spin alignments by using the nearby disk galaxies from the seventh data release of the Sloan Digital Sky Survey (SDSS DR7) (Abazajian et al. 2009). They showed that the galaxies which have ten or more neighbors within separation distance of $2 h^{-1}\text{Mpc}$ exhibit stronger spin-spin alignments. If the intrinsic spin-spin alignments were related to the tidally induced spin-shear alignments (e.g., Pen et al. 2000; Crittenden et al. 2001, 2002; Jing 2002; Mackey et al. 2002; Porciani et al. 2002a,b), this observational finding of Lee (2011) should be interpreted as another evidence for the stronger spin-shear alignments in denser environments, consistent with the result of Lee & Erdogdu (2007). Although Lee (2011) attempted to explain the observed environmental dependence of the intrinsic spin-spin alignments in the tidal torque picture, ascribing it to the dependence of the tidal strength on the local density, it remains unanswered why and how the initially established spin-shear alignments survive better in denser environments.

Several literatures have also suggested that the tidal torque theory alone could not provide a fully satisfactory explanation for the observed dependence of the galaxy intrinsic

alignments on the cosmic web environment (see, e.g., Hahn et al. 2007b; Jones et al. 2010; Codis et al. 2012; Libeskind et al. 2012a; Giahi & Schäfer 2013; Trowland et al. 2013). The general consensus reached by the previous numerical works is that the observed galaxy intrinsic alignments are not just weakened version of the initial spin-shear correlations but evolved version driven by some other mechanism than the tidal shears. What has so far suggested as a possible candidate for the required mechanism in the literatures includes the large-scale cosmic flow, peculiar motions, satellite infalls, bulk flows and etc.

Very recently, Libeskind et al. (2012b) proposed an interesting new scenario that the cosmic vorticity drives the nonlinear evolution of the galaxy angular momentum after the turn-around moments. In the linear regime the peculiar velocity field is curl free as it is described as a gradient of the perturbation potential. In the subsequent nonlinear evolution, however, it develops the curl mode which could affect the galaxy angular momentum. By analyzing the data from high-resolution N-body simulations, Libeskind et al. (2012b) demonstrated that the halo angular momentum vectors are strongly aligned with the local vorticity vectors, indicating the presence of the dominant effect of the vorticity field on the nonlinear evolution of the galaxy angular momentum vectors. The Libeskind et al. (2012b) also showed that the vorticity vectors are strongly anti-aligned with the major (minor) principal axes of the local tidal shear fields in the knot (void) environments.

We note here that the puzzling environmental dependence of the galaxy spin alignments can be coherently explained by assuming the vorticity driven evolution of the galaxy angular momentum. The goal of this Paper is to look for an observational evidence for this new scenario of Libeskind et al. (2012b). To achieve this goal, we reconstruct the cosmic vorticity and the galaxy spin fields from the large galaxy surveys and investigate if the vorticity-spin and vorticity-shear alignments found in N-body simulations exist in the real Universe. The upcoming three sections present the following highlights, respectively: the procedure to reconstruct the cosmic vorticity field and the result on the vorticity-shear alignments in section 2; a brief review of the algorithm to measure the galaxy spin axes with high accuracy and the result on the vorticity-spin alignments in section 3; a concise summary of the final results and discussion of the cosmological implication of our results in section 4.

2. VORTICITY-SHEAR ALIGNMENTS

Erdoğdu et al. (2006) reconstructed the density contrast $\delta(\mathbf{x})$ and peculiar velocity $\mathbf{v}(\mathbf{x})$ fields by applying the Wiener reconstruction algorithm to the galaxy data from the 2MASS redshift survey (Huchra et al. 2005) under the assumption of a Λ CDM universe. The fields were provided on 64^3 pixels in a regular cubic space of linear size $400 h^{-1}\text{Mpc}$, for which the

position vectors \mathbf{x} were expressed in the supergalactic coordinate system and the peculiar velocities \mathbf{v} were measured in the cosmic microwave background (CMB) frame. Given the spatial resolution of $6.25 h^{-1}\text{Mpc}$, the reconstructed fields represented the density and velocity fluctuations on the quasi-nonlinear scale. Erdoğdu et al. (2006) proved the robustness of their reconstruction procedure by demonstrating that the predicted density field recovers well the observed large scale structures of the Universe.

Using the density field $\delta(\mathbf{x})$ reconstructed by Erdoğdu et al. (2006) from the 2MASS redshift survey, Lee & Erdoğdu (2007) calculated the tidal fields as $T_{ij}(\mathbf{x}) = \partial_i \partial_j \nabla^{-1} \delta(\mathbf{x})$. Given that on those pixel points more distant than $100 h^{-1}\text{Mpc}$ from the center the reconstructed density and velocity fields suffered from large uncertainties (private communication with P.Erdoğdu), Erdoğdu et al. (2006) selected only those 32^3 pixels whose separation distances from the center are less than $100 h^{-1}\text{Mpc}$ and determined the major, intermediate and minor principal axes of $T_{ij}(\mathbf{x})$ at each selected pixel point. The detailed descriptions of the reconstructed density, velocity and tidal fields, and the 2MASS redshift survey can be found in Erdoğdu et al. (2006), Lee & Erdoğdu (2007) and Huchra et al. (2005), respectively.

Now, we attempt to reconstruct the cosmic vorticity field on the selected 32^3 pixel points by calculating the curl of the peculiar velocity field as $\mathbf{w} \equiv \nabla \times \mathbf{v}$. We first perform the Fourier transform of the peculiar velocity field to obtain its Fourier amplitudes $\tilde{\mathbf{v}}$ with the help of the Fast Fourier Transformation (FFT) code (Press et al. 1992). The Fourier amplitude of the vorticity field can be written as $\tilde{\mathbf{w}} = \mathbf{k} \times \tilde{\mathbf{v}}$ where \mathbf{k} is the wave vector in the Fourier space, and thus the three components of $\tilde{\mathbf{w}}$ are calculated in Fourier space as

$$\tilde{w}_1 = k_2 \tilde{v}_3 - k_3 \tilde{v}_2, \quad \tilde{w}_2 = k_3 \tilde{v}_1 - k_1 \tilde{v}_3, \quad \tilde{w}_3 = k_1 \tilde{v}_2 - k_2 \tilde{v}_1. \quad (1)$$

Finally, we perform the inverse Fourier transform of $\tilde{\mathbf{w}}$ to obtain the real-space vorticity field \mathbf{w} . Figure 1 plots the contours of the absolute magnitude of \mathbf{w} in the supergalactic x - y plane, showing the deviation of $|\mathbf{w}|$ from zero. Recalling the fact that the peculiar velocity field reconstructed from the 2MASS redshift survey was filtered on the quasi-nonlinear scale of $\sim 6.25 h^{-1}\text{Mpc}$, the result shown in Figure 1 implies that even in the quasi-nonlinear regime the velocity field is no longer irrotational, developing the curl mode.

As done in Libeskind et al. (2012b), we first divide the 32^3 pixels into the knots, filaments, sheets and voids according to the signs of the shear eigenvalues (Hahn et al. 2007a): The pixels at which all three eigenvalues have positive (negative) values are marked as knots (voids), while the pixels at which one eigenvalue is negative (positive) and the other two are positive (negative) are marked as filaments (sheets). Then, we calculate the alignment between the vorticity vector and the principal axes of the tidal tensor at each marked pixel. Let $\{\mathbf{e}_1, \mathbf{e}_2, \mathbf{e}_3\}$ be the major, intermediate and minor principal axes of the tidal tensor at each marked pixel. Calculating $\mu \equiv |\mathbf{w} \cdot \mathbf{e}_i|$ (for $i = 1, 2, 3$) and binning the values of μ in

the range of $[0, 1]$, we determine the probability density distribution of μ . If there were no alignment, the distribution $p(\mu)$ would be uniformly unity. If $p(\mu)$ increases (decreases) with μ , then there should be strong alignments (anti-alignments) between the vorticity vectors and the principal axes of the tidal tensors. We repeat the same calculation for the knot, void, filament and sheet regions to separately determine $p(\mu)$ for each case.

Figure 2 plots the probability density distributions, $p(\mu)$, with Poisson errors for the knot regions, showing how the vorticity vectors are aligned with the major, intermediate and minor principal axes of the tidal tensors in the left, middle and right panels, respectively. In each panel the horizontal dotted line indicates the uniform distribution of μ for the case of no vorticity-shear alignments. As can be seen, the vorticity vectors are strongly anti-aligned with the major principal axes of the tidal shear tensors, preferentially lying in the plane spanned by their intermediate and minor principal axes in the knot regions. In other words, in the highly dense knot environments the vorticity vectors are anti-aligned with the directions of the maximum matter compression.

Figure 3 plots $p(\mu)$ for the void regions, revealing that in the void regions the vorticity vectors are anti-aligned with the minor principal axes of the tidal tensors, preferentially lying in the plane spanned by the major and intermediate principal axes, which is directly opposite to the case of the knot regions. This result is consistent with the numerical finding of Libeskind et al. (2012b) even though in their work the vorticity field was filtered on much smaller scale. Figures 5 and 4 plot $p(\mu)$ for the filament and sheet cases, respectively. As can be seen, the filament regions show no strong signal of vorticity-shear alignments, while for the sheet case is found a clear signal alignments (anti-alignments) with the major (minor) principal axes but no strong alignments with the intermediate principal axes.

3. VORTICITY-SPIN ALIGNMENTS

The galaxy spin axes are hard to determine in practice, even under the simplified assumption that the minor axes of the galaxies are aligned with their spin axes. In the measurements of the alignments between the galaxy spin axes and the local vorticity vectors, the largest uncertainty would come from the inaccurate determination of the galaxy spin axes. Therefore, it is important to select carefully only those galaxies whose spin orientations can be determined with relatively high accuracy. It is often assumed that for the case of the late-type spiral galaxies whose shapes are close to circular thin discs their spin axes are orthogonal to the disc planes (Haynes & Giovanelli 1984). Provided that information on the position angles and axial ratios of the late-type spiral galaxies are available, their unit spin vectors can be determined up to the two-fold ambiguity in the sign of their radial

components (Pen et al. 2000). The remaining uncertainty due to this two-fold ambiguity in the determination of the spin axes can be minimized by considering only those face-on or edge-on spirals.

As it is essential for our investigation to determine the directions of the galaxy angular momentum vectors as accurately as possible, we restrict our analysis only to the nearby large late-type spiral galaxies viewed either face on or edge on. A sample of the nearby large late-type spiral galaxies was already obtained by Lee (2011) from the SDSS DR7. The sample contains those SDSS galaxies which have type Scd on the Hubble sequence (Huertas-Company et al. 2011), angular sizes larger than $D_c = 7.92$ arcseconds in the redshift range of $0 \leq z \leq 0.02$. The value of this size cut-off D_c was imposed to remove the dwarfs which turned out to cause large uncertainties in the measurements of the spin axes due to their irregular shapes. Among the nearby large Scd galaxies in the sample of Lee (2011), we make a further selection of only those ones which have axial ratios larger than 0.9 (nearly face-on) or smaller than 0.15 (nearly edge-on) to minimize the uncertainties associated with the two-fold ambiguity. A total of 585 nearby large late-type face-on (or edge-on) spirals are finally selected for our analysis.

The unit spin vector of each selected galaxy, $\hat{\mathbf{t}} \equiv (\hat{t}_x, \hat{t}_y, \hat{t}_z)$, is determined as (Lee 2011)

$$\hat{t}_x = \pm \cos \xi \sin(\pi/2 - \delta) \cos \alpha + |\sin \xi| \sin P \cos(\pi/2 - \delta) \cos \alpha - |\sin \xi| \cos P \sin \alpha, \quad (2)$$

$$\hat{t}_y = \pm \cos \xi \sin(\pi/2 - \delta) \sin \alpha + |\sin \xi| \sin P \cos(\pi/2 - \delta) \sin \alpha + |\sin \xi| \cos P \cos \alpha, \quad (3)$$

$$\hat{t}_z = \pm \cos \xi \cos(\pi/2 - \delta) - |\sin \xi| \sin P \sin(\pi/2 - \delta), \quad (4)$$

where P is the position angle of each selected galaxy, and (δ, α) are the declination and right ascension of each galaxy's position vector expressed in the equatorial coordinate system, and the plus and minus signs in front of the first terms in Equation (2)-(4) represents the two-fold ambiguity mentioned above. Here, ξ is the galaxy's inclination angle related to its axial ratio q and intrinsic flatness parameter p as $\cos^2 \xi = (q^2 - p^2)(1 - p^2)$. For the galaxies of type Scd, the intrinsic flatness parameter has the value of $p = 0.1$ (Haynes & Giovanelli 1984). Since the tidal shear and the vorticity fields from the 2MASS redshift survey have been reconstructed in the super-galactic coordinate systems, we find a supergalactic expression for the unit spin vector of each selected galaxy, $\hat{\mathbf{s}}$, through the coordinate transformation of $\hat{\mathbf{s}} = R\hat{\mathbf{t}}$ where R is the orthogonal matrix that transforms the equatorial to the supergalactic frames.

By applying the Cloud-in-Cell interpolation (CIC) algorithm (Hockney & Eastwood 1988) to the tidal shear fields reconstructed by Lee & Erdogdu (2007) from the 2MASS redshift survey, we determine the tidal shear tensors at the positions of the selected SDSS

galaxies and determine their principal axes, $\{\mathbf{e}_1, \mathbf{e}_2, \mathbf{e}_e\}$. Then, we calculate the cosines of the alignment angles, μ , between the galaxy spin axes and the principal axes of the local tidal tensors as $\mu \equiv |\mathbf{s} \cdot \mathbf{e}_i|$. Recall that there are two different unit spin vectors assigned to each selected galaxy which differ from each other by the sign of the radial components. As done in Lee & Erdoğdu (2007), we treat two spin vectors assigned to each galaxy as two independent realizations to end up having twice as many values of μ as the total number of the selected SDSS galaxies. Binning the values of μ and counting the number of those realizations, n_μ , belonging to each μ -bin, we finally determine the probability density distribution, $p(\mu)$, of the spin-shear alignments, calculating Poisson errors as $1/(n_\mu - 1)^{1/2}$ associated with the determination of $p(\mu)$.

Figure 6 plots the probability density distributions of the cosines of the alignment angles between the unit spin vectors of the selected SDSS galaxies and the major, intermediate, and minor principal axes of the local tidal shear tensors with Poisson errors in the left, middle and right panels, respectively. As can be seen, the spin axes of the selected galaxies seem to be strongly anti-aligned with the major principal axes of the local tidal tensors, but aligned with the intermediate and the minor principal axes. That is, the spin axes of the selected SDSS galaxies tend to lie in the plane perpendicular to the local direction of maximum matter compression.

Compare our result with that of Lee & Erdoğdu (2007) who found a significant signal of the correlations between the spin axes of the Tully galaxies and the intermediate principal axes of the local tidal tensors but no alignment signal with the other two principal axes. We believe that the difference resulted from the inaccurate measurements of the spin axes of the Tully galaxies in the analysis of Lee & Erdoğdu (2007) which included not only the Scd galaxies but also the earlier type spirals with thick bulges without taking into account the two-fold ambiguity. What is newly found from our analysis is that the anti-alignments between the spin axes and the major principal axes are strongest while the alignments of the spin axes with the minor principal axes are as strong as that with the intermediate principal axes. Although the result is not completely against the tidal torque theory which predicts that the spin axes are preferentially aligned with the intermediate principal axes, we would like to see if there exists strong spin-vorticity alignments which may help explain better the detected spin-shear alignment tendency.

Applying the CIC algorithm to the vorticity fields reconstructed in section 2, we calculate the local vorticity vectors at the positions of the selected SDSS disk galaxies. Then, we determine the probability distribution of the cosines of the angles between the unit spin vectors and the local vorticity vectors \mathbf{w} in a similar manner, the result of which is plotted Figure 7. As can be seen, the probability density increases sharply and almost monotonically

as μ increases, detecting a strong signal of the spin-vorticity alignments. We test the null hypothesis of no alignment (i.e., $p(\mu) = 1$) with the help of the χ^2 -statistics and find that the null hypothesis is rejected at the 99.9999% confidence level.

The result shown in Figure 7 is consistent with the numerical finding of Libeskind et al. (2012b), providing an observational support for the scenario that the galaxy angular momentum evolves via its interaction with the local vorticity in the nonlinear regime. Recalling that in the work of Libeskind et al. (2012b) the vorticity field was filtered on the galactic scale of $\leq 1^{-1} h^{-1} \text{Mpc}$ while in the current work the vorticity field is filtered on the much larger scale of $\sim 6 h^{-1} \text{Mpc}$, we conclude that the vorticity effect wins over the tidal shear effect on the evolution of the galaxy angular momentum even in the quasi-nonlinear regime.

4. SUMMARY AND DISCUSSION

Utilizing the nearby large face-on (or edge-on) late-type spiral galaxies from the SDSS DR7 (Abazajian et al. 2009) and the tidal shear and vorticity fields reconstructed from the 2MASS redshift survey (Erdoğdu et al. 2006), we have measured the vorticity-shear, the spin-shear and the spin-vorticity alignments. The reconstructed vorticity fields have spatial resolution of $\sim 6 h^{-1} \text{Mpc}$, corresponding to the quasi-nonlinear regime. First, the vorticity vectors have been found to be strongly anti-aligned (aligned) with the major principal axes of the tidal shear tensors in the knot (void) regions, lying in the plane spanned by the other two principal axes. Second, the galaxy spin axes have turned out to be strongly anti-aligned with the major principal axes of the local tidal shear tensors, while aligned with the intermediate and minor principal axes. Finally, a clear signal of the spin-vorticity alignments has been detected, rejecting the null hypothesis of no spin- vorticity alignment at 99.9999% significance level. This result observationally stands by the new scenario of Libeskind et al. (2012b) that the tidally generated angular momentum of a galaxy subsequently evolves under the dominant effect of the vorticity field in the quasi-nonlinear and nonlinear regime.

The spin-shear alignment tendency as well as its environmental dependence reported in the previous works can now be explained as follows. The cosmic flow in the nonlinear regime develops local vorticities which are preferentially inclined onto the plane orthogonal to the directions of either the maximum or the minimum volume compression depending on the web environment. The developed vorticities affect the galaxy angular momentum, modifying the spin-shear alignments from the initial tendency. Since it depends on the environment how fast the velocity field develops the vorticities and what directions the vorticity vectors get aligned with, the spin-shear alignments in the nonlinear regime come to take on the environmental dependence. The stronger spin-shear alignments found in denser environments should result

from the stronger vorticity effect there via which the nonlinear spin-shear alignments are established.

An interesting cosmological implication of our result is that the nonlinear vorticity fields and the the vorticity-induced galaxy alignments might be useful as a probe of cosmology and gravity. As shown in Kitaura et al. (2012) and mentioned in Libeskind et al. (2012b), the vorticity of cosmic fluid which equals zero in the linear regime grows in the nonlinear regime at third order. The more rapidly a cosmic fluid develops the third order nonlinearity, the stronger the spin-vorticity alignments become due to the earlier onset of the vorticity effect on the evolution of the galaxy angular momentum. In some modified gravity or dynamic dark energy models the high-order nonlinearity grows faster due to the presence of the fifth force than for the Λ CDM case. Thus, in these alternative models the faster growth of the nonlinearity would lead to the more rapid development of the vorticity field, generating stronger spin-vorticity alignments. Very recently, Li et al. (2013) claimed that the small scale powers of the divergence of the peculiar velocities should be a more sensitive probe of modified gravity than the density power spectrum. Given our result, the small-scale powers of the absolute magnitude of the curl of the peculiar velocities might work powerfully as a complimentary probe.

I thank P.Erdogdu for providing me the data of the density and peculiar velocity fields from the 2MASS redshift survey. I also thank M. Huertas-Company for providing information on the galaxy position angles and magnitudes. This work was supported by the National Research Foundation of Korea (NRF) grant funded by the Korea government (MEST, No.2012-0004195). Support for this work was also provided by the National Research Foundation of Korea to the Center for Galaxy Evolution Research (NO. 2010-0027910). Funding for the SDSS and SDSS-II has been provided by the Alfred P. Sloan Foundation, the Participating Institutions, the National Science Foundation, the U.S. Department of Energy, the National Aeronautics and Space Administration, the Japanese Monbukagakusho, the Max Planck Society, and the Higher Education Funding Council for England. The SDSS Web Site is <http://www.sdss.org/>. The SDSS is managed by the Astrophysical Research Consortium for the Participating Institutions. The Participating Institutions are the American Museum of Natural History, Astrophysical Institute Potsdam, University of Basel, University of Cambridge, Case Western Reserve University, University of Chicago, Drexel University, Fermi lab, the Institute for Advanced Study, the Japan Participation Group, Johns Hopkins University, the Joint Institute for Nuclear Astrophysics, the Kavli Institute for Particle Astrophysics and Cosmology, the Korean Scientist Group, the Chinese Academy of Sciences (LAMOST), Los Alamos National Laboratory, the Max-Planck-Institute for Astronomy (MPIA), the Max-Planck-Institute for Astrophysics (MPA), New Mexico State University, Ohio State Univer-

sity, University of Pittsburgh, University of Portsmouth, Princeton University, the United States Naval Observatory, and the University of Washington.

REFERENCES

- Abazajian, K. N., Adelman-McCarthy, J. K., Agüeros, M. A., et al. 2009, *ApJS*, 182, 543
- Catelan, P., & Theuns, T. 1996, *MNRAS*, 282, 436
- Catelan, P., & Theuns, T. 1996, *MNRAS*, 282, 455
- Codis, S., Pichon, C., Devriendt, J., et al. 2012, *MNRAS*, 427, 3320
- Crittenden, R. G., Natarajan, P., Pen, U.-L., & Theuns, T. 2001, *ApJ*, 559, 552
- Crittenden, R. G., Natarajan, P., Pen, U.-L., & Theuns, T. 2002, *ApJ*, 568, 20
- Doroshkevich, A. G. 1970, *Astrofizika*, 6, 581
- Dubinski, J. 1992, *ApJ*, 401, 441
- Erdoğdu, P., Lahav, O., Huchra, J. P., et al. 2006, *MNRAS*, 373, 45
- Giahi, A., & Schäfer, B. M. 2013, *MNRAS*, 428, 1312
- Hahn, O., Porciani, C., Carollo, C. M., & Dekel, A. 2007, *MNRAS*, 375, 489
- Hahn, O., Carollo, C. M., Porciani, C., & Dekel, A. 2007, *MNRAS*, 381, 41
- Haynes, M. P., & Giovanelli, R. 1984, *AJ*, 89, 758
- Hockney, R. W., & Eastwood, J. W. 1988, (Bristol: Hilger)
- Huchra, J., Jarrett, T., Skrutskie, M., et al. 2005, *Nearby Large-Scale Structures and the Zone of Avoidance*, 329, 135
- Huertas-Company, M., Aguerri, J. A. L., Bernardi, M., Mei, S., & Sánchez Almeida, J. 2011, *A&A*, 525, A157
- Jing, Y. P. 2002, *MNRAS*, 335, L89
- Jones, B. J. T., van de Weygaert, R., & Aragón-Calvo, M. A. 2010, *MNRAS*, 408, 897
- Kitaura, F.-S., Angulo, R. E., Hoffman, Y., & Gottlöber, S. 2012, *MNRAS*, 425, 2422
- Lee, J., & Erdoğdu, P. 2007, *ApJ*, 671, 1248
- Lee, J., & Park, D. 2006, *ApJ*, 652, 1
- Lee, J. & Pen, U. L. 2000, *ApJ*, 532, L5

- Lee, J. & Pen, U. L. 2001, *ApJ*, 555, 106
- Lee, J., & Pen, U.-L. 2002, *ApJ*, 567, L111
- Lee, J. & Erdogdu, P. 2007, 671, 1248
- Lee, J., & Pen, U.-L. 2008, *ApJ*, 681, 798
- Lee, J. 2011, *ApJ*, 732, 99
- Li, B., Hellwing, W. A., Koyama, K., et al. 2013, *MNRAS*, 428, 743
- Libeskind, N. I., Hoffman, Y., Knebe, A., et al. 2012, *MNRAS*, 421, L137
- Libeskind, N. I., Hoffman, Y., Steinmetz, M., et al. 2012, *arXiv:1212.1454*
- Mackey, J., White, M., & Kamionkowski, M. 2002, *MNRAS*, 332, 788
- Navarro, J. F., Abadi, M. G., & Steinmetz, M. 2004, *ApJ*, 613, L41
- Patiri, S. G., Cuesta, A. J., Prada, F., Betancort-Rijo, J., & Klypin, A. 2006, *ApJ*, 652, L75
- Peebles, P. J. E. 1969, *ApJ*, 155, 393
- Pen, U.-L., Lee, J., & Seljak, U. 2000, *ApJ*, 543, L107
- Pichon, C., & Bernardeau, F. 1999, *A&A*, 343, 663
- Porciani, C., Dekel, A., & Hoffman, Y. 2002, *MNRAS*, 332, 325
- Porciani, C., Dekel, A., & Hoffman, Y. 2002, *MNRAS*, 332, 339
- Press, W. H., Teukolsky, S. A., Vetterling, W. T. & Flannery, B. P. 1992, *Numerical Recipes in FORTRAN* (Cambridge : Cambridge Univ. Press)
- Schäfer, B. M. 2009, *International Journal of Modern Physics D*, 18, 173
- Schäfer, B. M., & Merkel, P. M. 2012, *MNRAS*, 421, 2751
- Trowland, H. E., Lewis, G. F., & Bland-Hawthorn, J. 2013, *ApJ*, 762, 72
- van den Bosch, F. C., Abel, T., Croft, R. A. C., Hernquist, L., & White, S. D. M. 2002, *ApJ*, 576, 21
- White, S. D. M. 1984, *ApJ*, 286, 38

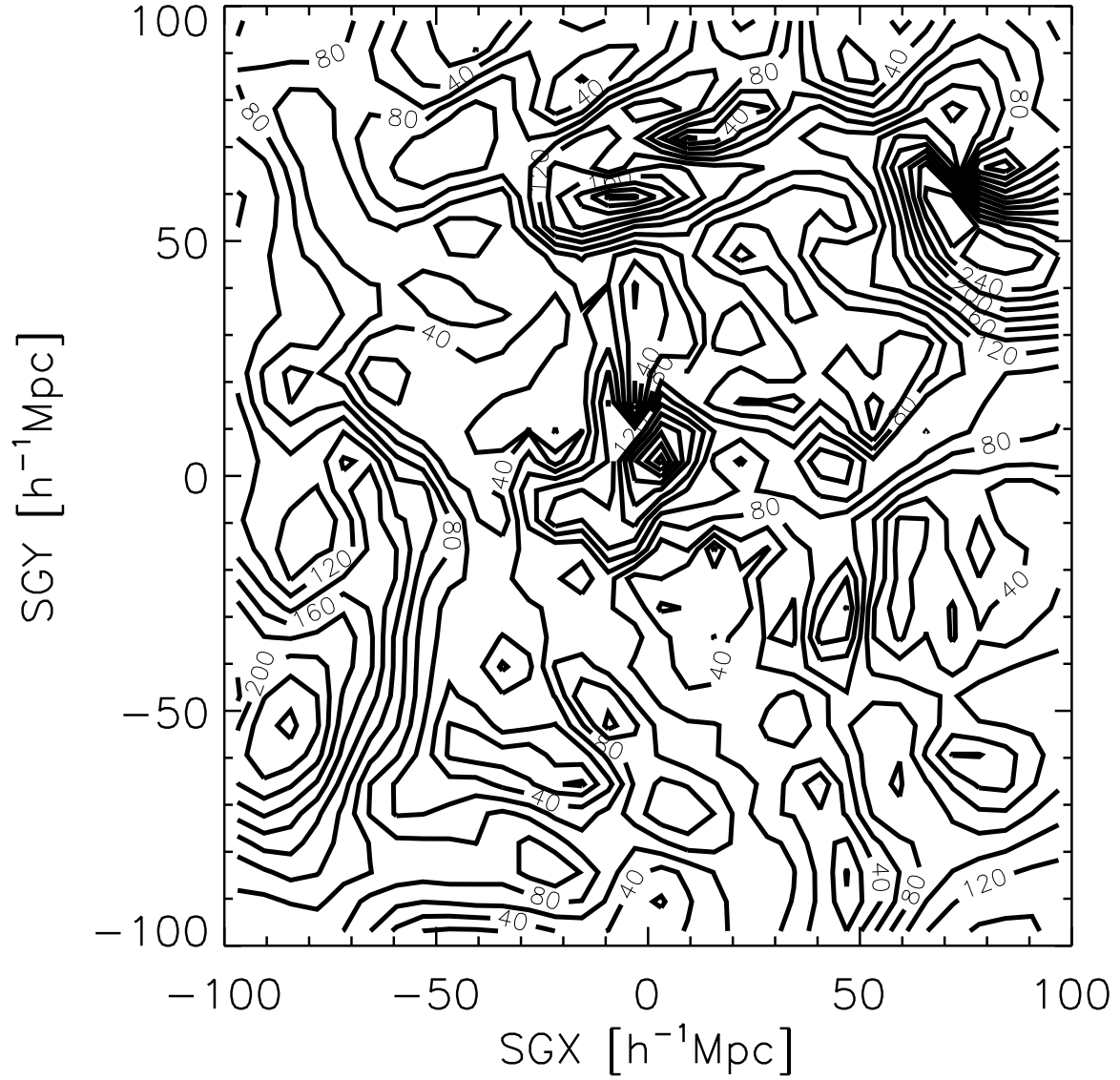


Fig. 1.— Contours of the magnitudes of the real space vorticity fields reconstructed from the 2MASS redshift survey in the supergalactic x - y plane.

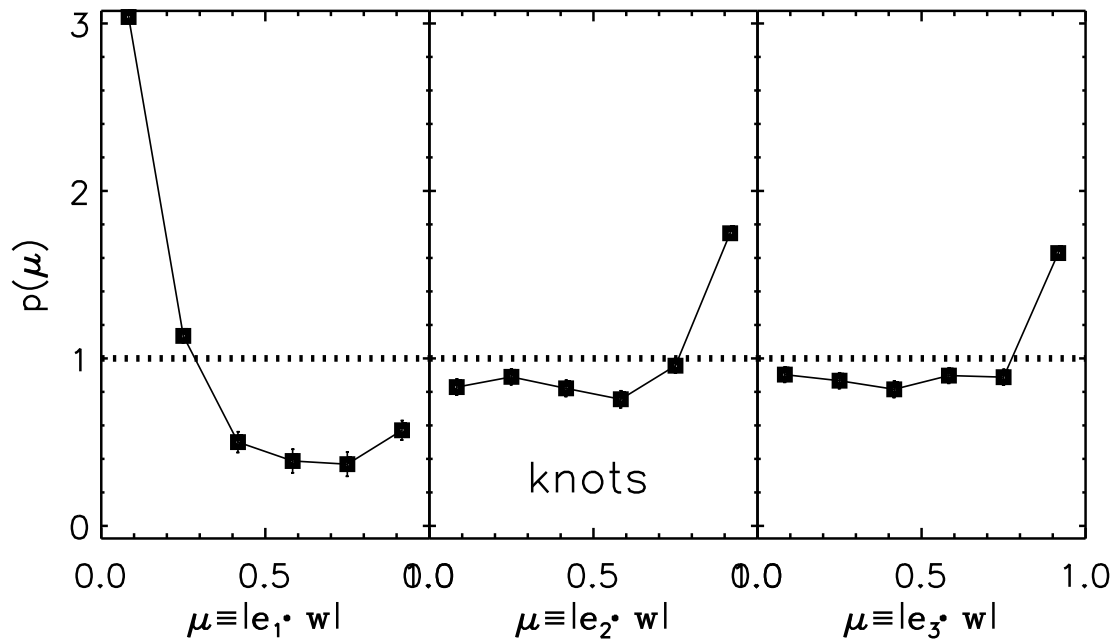


Fig. 2.— Probability density distributions of the cosines of the angles between the vorticity vectors and the major, intermediate and minor principal axes of the tidal shear tensors in the left, middle and right panels, respectively, for the knot regions where the eigenvalues of the tidal shear tensors are all positive. In each panel, the dotted line corresponds to the case of no alignment and the errors are Poissonian.

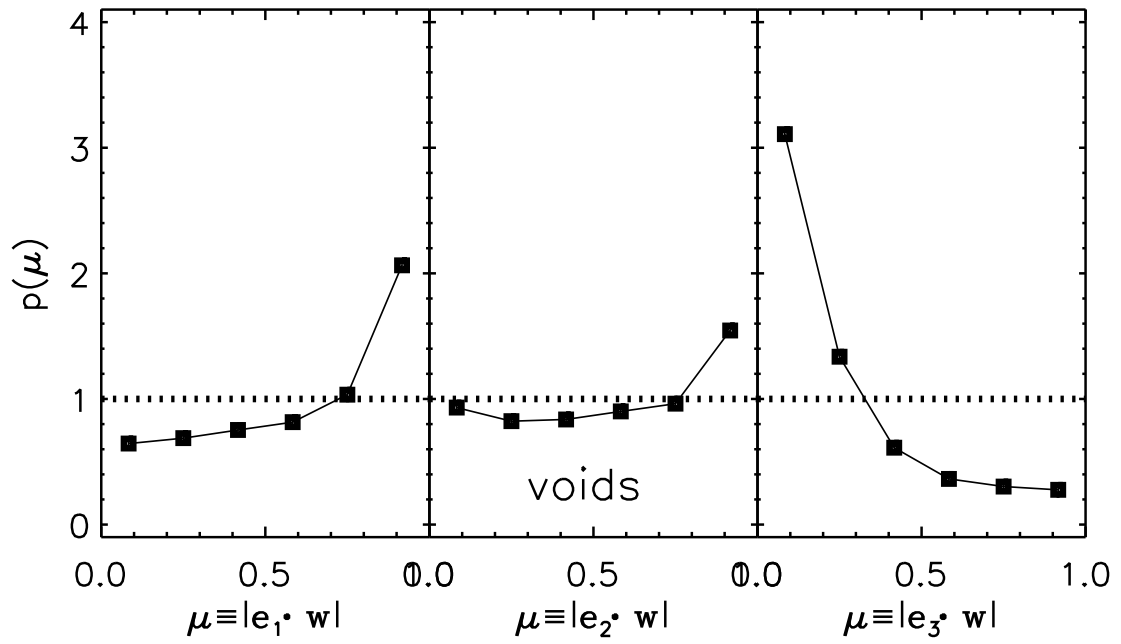


Fig. 3.— Same as Figure 2 but for the void regions where the shear eigenvalues are all negative.

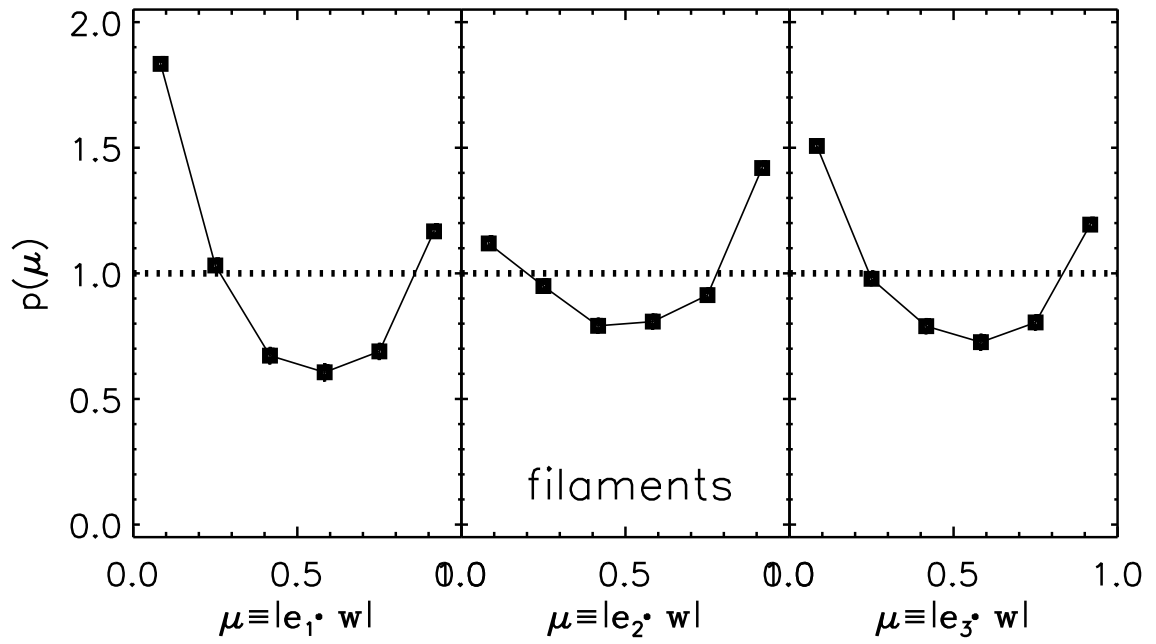


Fig. 4.— Same as Figure 2 but for the filament regions that the largest and second to the largest shear eigenvalues are positive while the smallest eigenvalues are negative.

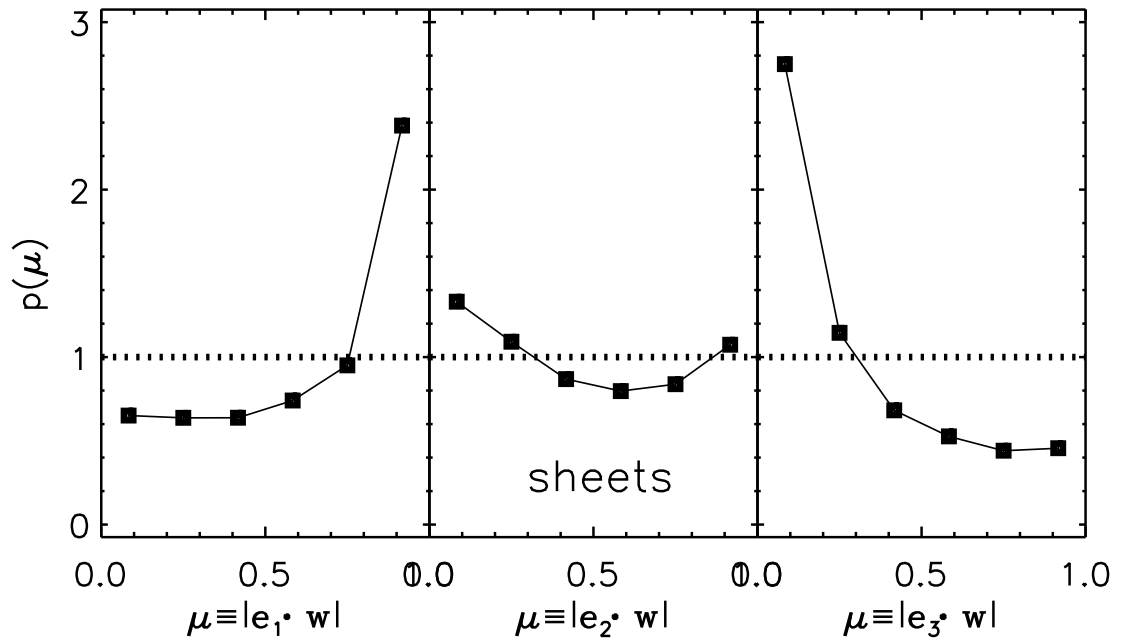


Fig. 5.— Same as Figure 2 but for the sheet regions that the smallest shear eigenvalues are negative while the other two shear eigenvalues are positive.

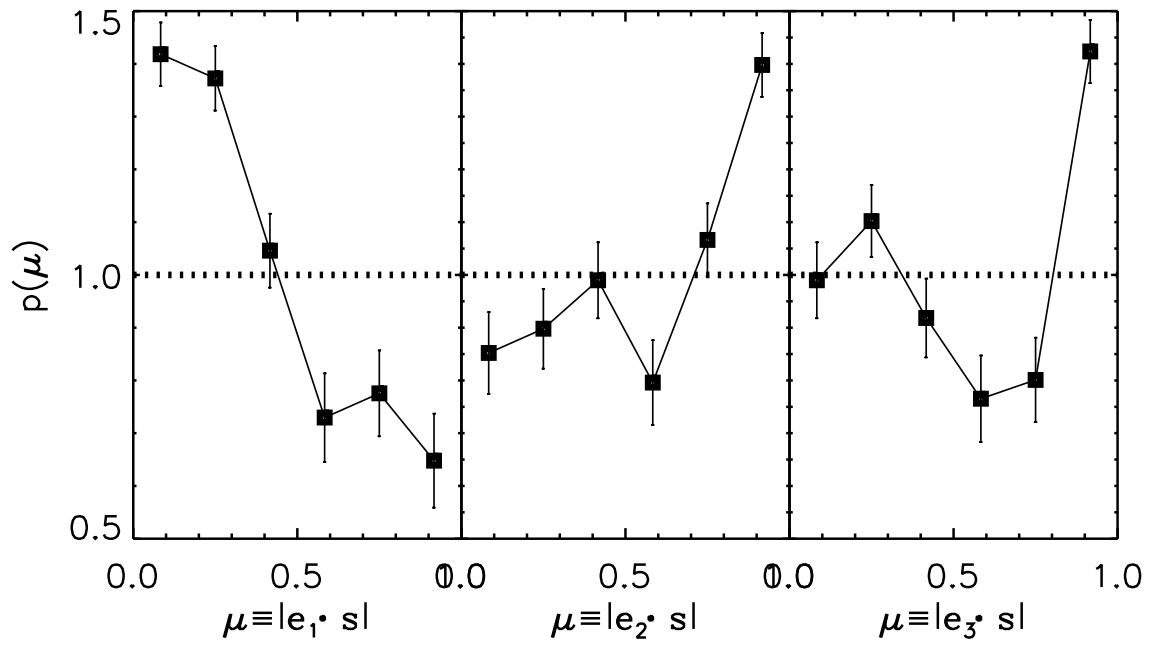


Fig. 6.— Probability density distributions of the cosine of the angles between the the galaxy spin vectors and the major, intermediate and minor principal axes of the tidal shear tensors with Poisson errors in the left, middle and right panels, respectively.

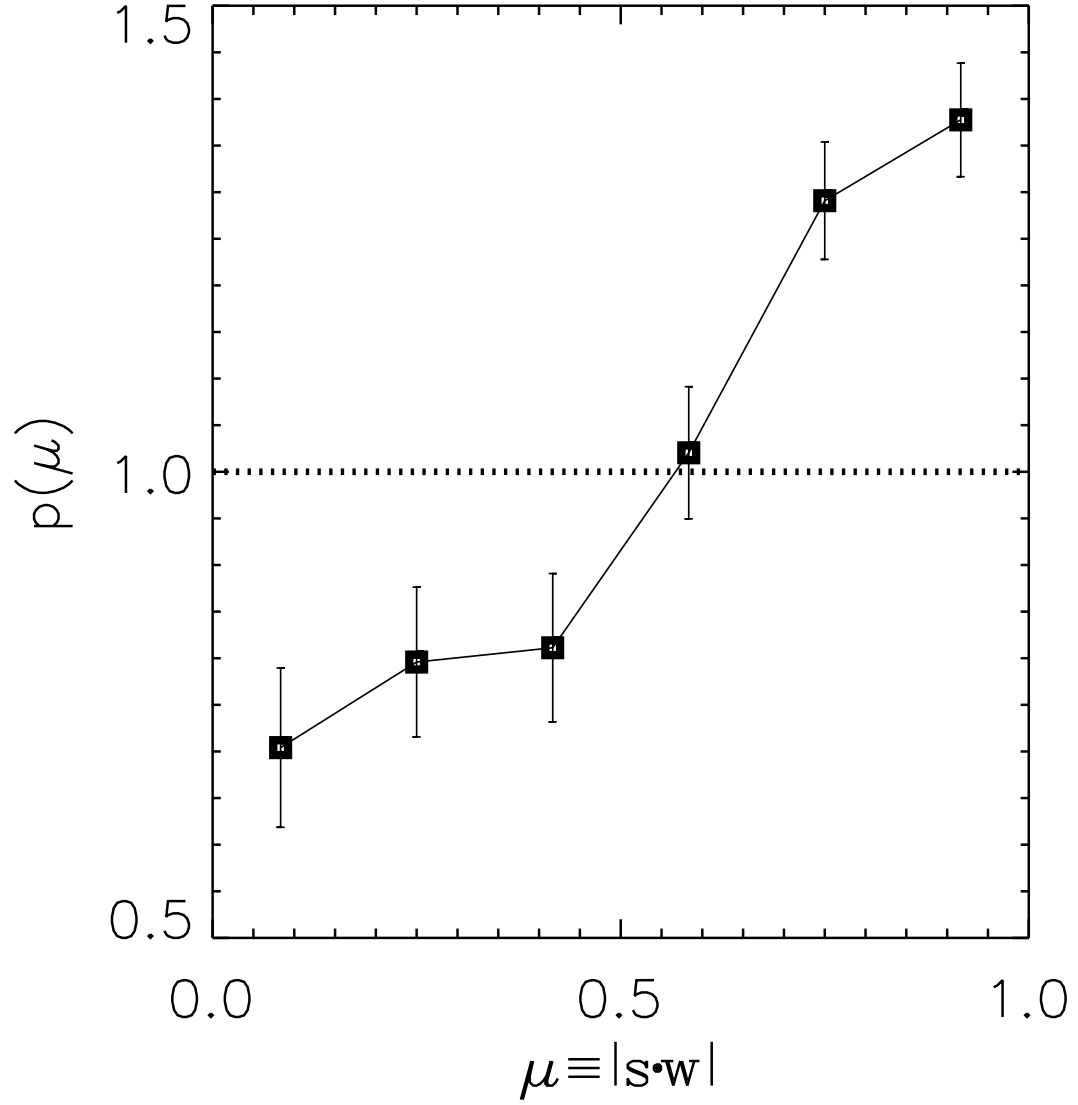


Fig. 7.— Probability density distribution of the cosines of the angles between the vorticity vectors and the spin vectors of the nearby large face-on (or edge-on) Scd galaxies selected from the SDSS DR7 with Poisson errors.